

FROM THIN TO THICK: THE IMPACT OF X-RAY IRRADIATION ON ACCRETION DISKS IN AGN

PHILIP CHANG^{1,2}, ELIOT QUATAERT¹, AND NORMAN MURRAY^{3,4}

Draft version September 21, 2017

ABSTRACT

We argue that the X-ray and UV flux illuminating the parsec-scale accretion disk around luminous active galactic nuclei (AGN) is super-Eddington with respect to the local far-infrared dust opacity. The far infrared opacity may be larger than in the interstellar medium of the Milky Way due to a combination of supersolar metallicity and the growth of dust grains in the dense accretion disk. Because of the irradiating flux, the outer accretion disk puffs up with a vertical thickness $h \sim R$. This provides a mechanism for generating a geometrically thick obscuring region from an intrinsically thin disk. We find obscuring columns $\sim 10^{22} - 10^{23} \text{ cm}^{-2}$, in reasonable agreement with observations.

Subject headings: galaxies: active – galaxies: Seyfert – galaxies: nuclei – accretion, accretion disks – dust, extinction

1. INTRODUCTION

The Seyfert unification model postulates the existence of a dusty geometrically thick obscuring region (the “torus”) in order to account for many of the observed differences among various classes of AGN (Antonucci 1993). The large infrared fluxes from quasars also provide evidence for obscuration of the central source, with covering fractions of 10-50% (Sanders et al. 1989). Recent observations with SDSS have directly detected a large number of Type 2 (obscured) quasars (e.g. Zakamska et al. 2003, 2005; Ptak et al. 2006).

The origin of the geometrically thick obscuring material in AGN remains uncertain. The host galaxy may provide the obscuration as in the case of MCG-6-30-15 (Ballantyne, Weingartner, & Murray 2003). A warped disk is directly implicated in the low-luminosity AGN NGC 4258 (Greenhill et al. 1995) and may be relevant more generally (Sanders et al. 1989). Alternatively, the obscuring material may arise in an outflow from the underlying accretion disk (e.g., Konigl & Kartje 1994). Energy injection by star formation (e.g., Wada & Norman 2002; Thompson et al. 2005) or viscous stirring in a clumpy accretion disk (Krolik & Begelman 1988) may also help generate the large random motions necessary to maintain $h \sim r$. Lastly, Pier & Krolik (1992) pointed out that, for luminous AGN, radiation pressure from the central AGN could help maintain the vertical thickness of obscuring material.

In this paper, we present a model for how geometrically thick obscuring material might arise from X-ray illumination incident on an initially thin AGN disk (§ 2). This model is complementary to that of Pier & Krolik (1992); we focus on how X-ray irradiation can thicken an underlying thin disk, while they highlighted the importance of radiation pressure support for already geometrically thick material. In § 3, we argue that the far infrared

opacity in AGN disks is larger than that in the interstellar medium (ISM) of the Milky Way, which increases the dynamical importance of X-ray and UV irradiation. The dust opacity is enhanced due to 1. supersolar metallicity and 2. larger dust grains. We discuss the evolution of dust grains in AGN disks via accretion of metals from the gas and dust grain coagulation. We show that the conditions in a thin AGN disk appear conducive to grain growth (as also suggested by, e.g., Laor & Draine 1993 and Maiolino et al. 2001ab). Finally, in § 4 we discuss our results and their observational implications.

2. X-RAY HEATED AGN DISKS

Here we consider the impact of X-ray illumination on the structure of AGN disks. Our physical picture is as follows (see Fig. 1). UV and X-ray radiation from the central source are incident at a grazing angle on a region of a thin disk which has a thickness h/R . Due to the high opacity of dust to UV photons, the incident UV flux is absorbed well above the IR photosphere of the disk. UV irradiation thus tends to make the disk more isothermal and does not provide an internal radiation pressure gradient which can help support the disk. X-rays in the 10-100 keV range, on the other hand, are electron-scattered in the outer atmosphere of the disk with approximately half of the X-rays being downscattered. If the underlying accretion disk is sufficiently Compton thick, most of the downscattered X-rays lose their energy via Compton scattering below the IR photosphere. This energy is then re-radiated in the IR, diffuses towards the surface of the disk, and provides a radiation pressure gradient which is dynamically important if the energy deposition via X-rays is sufficiently high. We show that as a result of this X-ray irradiation, the entire disk cannot remain thin. Instead, the outer atmosphere puffs up to $h \sim R$ producing significant obscuration along most lines of sight. As discussed later in §4, our calculation does not quantitatively describe the final structure of the resulting geometrically thick atmosphere, which requires a multi-dimensional calculation that incorporates both UV and X-ray irradiation.

We now calculate the critical luminosity so that X-ray irradiation becomes dynamically important. The inci-

¹ Astronomy Department and Theoretical Astrophysics Center, 601 Campbell Hall, University of California, Berkeley, CA 94720; pchang@astro.berkeley.edu, eliot@astro.berkeley.edu

² Miller Institute for Basic Research

³ Canadian Institute for Theoretical Astrophysics, 60 St. George Street, University of Toronto, Toronto, ON M5S 3H8, Canada; murray@cita.utoronto.ca.

⁴ Canada Research Chair in Astrophysics

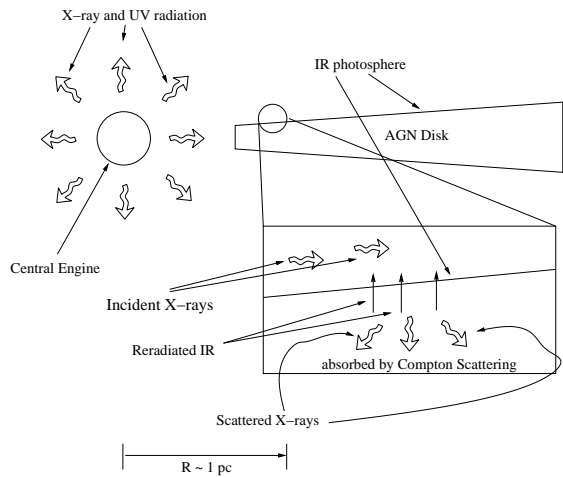


FIG. 1.— Schematic Diagram of an X-ray Illuminated AGN Disk

dent X-ray flux on the initially thin disk is

$$F_X = \frac{L_X}{4\pi R^2} \frac{h}{R}, \quad (1)$$

where L_X is the X-ray luminosity from the central source and R is the radius of the disk. The X-ray opacity is provided by electron scattering and photoionization. For X-ray energies above ≈ 10 keV, electron scattering dominates. At these energies, an x-ray photon incident on a disk with scale height h/R is scattered at a column of $1/\kappa_e(h/R)$, where κ_e is the electron scattering opacity. Since the scattering is roughly isotropic, half of the X-rays are scattered out to infinity and half are scattered downward into the disk. The half that are scattered downward heat the disk via photoionization and Compton scattering. We adopt the photoionization cross section from Maloney, Hollenbach, & Tielens (1996) which gives $\sigma = 4.4 \times 10^{-22} (E/1 \text{ keV})^{-8/3} \text{ cm}^2$ for $E > 7$ keV, where E is the energy of the X-ray photon. We calculate the efficiency of this heating for an incident spectrum typical of AGN (photon index $\alpha = 1.7$) as a function of depth and show the results in Figure 2. The total energy absorbed by the disk is a function of its Compton thickness, but above a total column, $y_{\text{tot}} = \int \rho dz$, of 20 g cm^{-2} , the heating saturates. For these columns, $\approx 2/3$ of the energy of the downward scattered X-rays heats the disk, with most of the energy being deposited in the first few Thomson depths. Models of accretion disks in luminous AGN predict surface densities of $\sim 10 - 10^3 \text{ g cm}^{-2}$ on parsec scales (Sirko & Goodman 2003; Thompson et al. 2005), so X-ray heating is expected to be quite important. These X-rays are reprocessed into the infrared where the opacity is substantial.

Under the conditions of interest, the radiation pressure gradient typically exceeds the gas pressure gradient near the IR photosphere. In order to support the photosphere to a height h , the IR flux, F_{IR} , through the disk must satisfy the dust Eddington limit ($F_{\text{IR}} \approx F_{\text{Edd,d}}$) or

$$F_{\text{IR}} \approx F_{\text{Edd,d}} = \frac{\Omega^2 h c}{\kappa_d}, \quad (2)$$

where κ_d is the dust IR opacity. Since the net flux radiated by the IR photosphere is due to the fraction of the incident X-ray flux deposited beneath the photosphere,

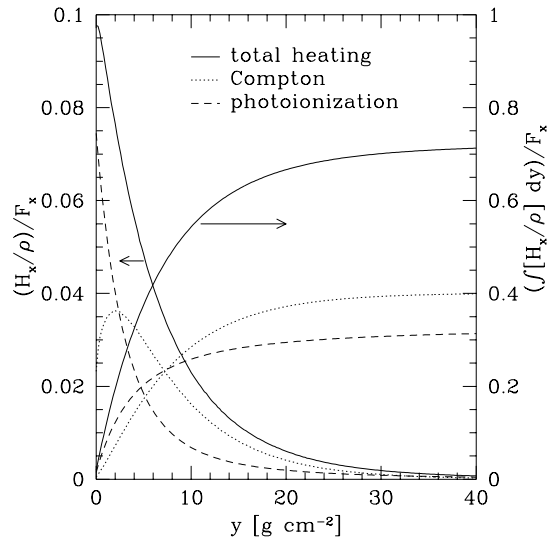


FIG. 2.— Local heating rate (H_x/ρ) per unit mass and integrated heating rate ($\int (H_x/\rho) dy$) as a function of column y (measured downward into the disk) for a slab irradiated by a power-law X-ray spectrum with a photon index of 1.7 and a high energy cutoff of 100 keV. Arrows indicate the vertical axis associated with each solid line. The heating rates are normalized to the total x-ray flux incident on the column (F_x) so that $(\int H_x dy)/F_x$ is the fraction of the incident flux that has been absorbed at a given depth y . The total heating rate, Compton scattering heating, and photoionization heating are given by the solid-lines, dotted lines and dashed lines, respectively.

we also have

$$F_{\text{IR}} = \epsilon \frac{L_X}{4\pi R^2} \frac{h}{R}, \quad (3)$$

where $\epsilon \approx 1/3$ is the efficiency with which X-ray flux is absorbed deep in the disk, which we estimate from the half of the X-rays that are downward scattered and the two-thirds of this energy that is absorbed. For a warped disk, all of the incident X-ray may heat the disk, not just the scattered radiation. Equating equations (2) and (3), we find a critical luminosity

$$L_{X, \text{crit}} = \epsilon^{-1} \frac{4\pi G M_{\text{BH}} c}{\kappa_d} = \epsilon^{-1} L_{\text{Edd}} \frac{\kappa_e}{\kappa_d}, \quad (4)$$

where $L_{\text{Edd}} = 4\pi G M_{\text{BH}} c / \kappa_e$ is the electron scattering Eddington limit and M_{BH} is the mass of the central black hole. For $L_X > L_{X, \text{crit}}$, the disk is locally unstable to puffing up because the energy deposited below the IR photosphere exceeds the local dust Eddington limit.

The critical luminosity $L_{X, \text{crit}}$ is sensitive to the details of the dust opacity in AGN disks through κ_e/κ_d . For the conditions of interest $T \sim 300 - 1000$, K and normal ISM dust is estimated to have a Rosseland mean opacity between $\kappa_d \approx 5$ (Semenov et al. 2003) and $\kappa_d \approx 15 \text{ cm}^2 \text{ g}^{-1}$ (Draine 2003). In the next section, we argue that the far infrared opacity in the near-AGN environment may be as large as $\kappa_d \sim 50 \text{ cm}^2 \text{ g}^{-1}$ due to increased metallicity and grain growth in AGN disks. In this case, $\kappa_e/\kappa_d \approx 0.01$ which in turn implies $L_{X, \text{crit}}/L_{\text{Edd}} \approx 0.03$. Bright Seyferts and quasars have X-ray luminosities that are roughly 0.01-0.1 of the (electron-scattering) Eddington luminosity, so a large number of systems are near the critical luminosity needed to have X-ray heating significantly affect the structure of a thin dusty parsec-scale

disk (§4).

To understand the impact of X-ray irradiation in more detail, we calculate the vertical structure of an irradiated thin disk. We begin with the equation of hydrostatic balance,

$$\frac{dP_{\text{gas}}}{dz} = -\rho \left(g - \frac{\kappa_d F}{c} \right), \quad (5)$$

and radiative balance,

$$\frac{dP_{\text{rad}}}{dz} = -\frac{\kappa_d F \rho}{c}, \quad (6)$$

where $P_{\text{gas}} = \rho k_B T / m_p$ is the gas pressure, T is the temperature, $P_{\text{rad}} = aT^4/3$ is the radiation pressure, F is the flux, z is the height defined from the midplane, $g = 2\pi G\Sigma + \Omega^2 z$ is the local gravitational acceleration, and $\Omega = \sqrt{GM_{\text{BH}}/R^3}$ is the local Keplerian frequency. Note we define the disk surface density $\Sigma = \int \rho dz = 0$ at the midplane here and is defined upward. For the Rosseland mean opacity of dust, we assume a simple model for numerical convenience: we take a constant value of $\kappa_d = 50 \text{ cm}^2 \text{ g}^{-1}$ between $T = 100 \text{ K}$ and $T = T_{\text{sub}} = 1500 \text{ K}$ (see eq. [17]). We model the rapid drop in opacity as the dust sublimates using $\kappa_d \propto \exp(-(T - T_{\text{sub}})/\Delta T)$ for $T > T_{\text{sub}}$, where $\Delta T \approx 100 \text{ K}$ defines the rough width of the transition. None of the qualitative features of our model depend on the choice of $\kappa_d = 50 \text{ cm}^2 \text{ g}^{-1}$ at low T , although the quantitative importance of irradiation does depend on the absolute normalization of κ_d (as discussed above in the context of $L_{X,\text{crit}}$).

The impact of X-ray heating on the structure of the disk can be modeled as a source term in the equation for the flux:

$$\frac{dF}{dz} = H(z) \quad (7)$$

where $H(z)$ is the heating function shown in Figure 2. To calculate the structure of the irradiated disk, we integrate equations (5), (6), and (7) from $z = 0$ to $z = z_0$, where z_0 is the IR photosphere. We enforce $F(z = 0) = 0$ at the midplane and the photospheric condition at $z = z_0$, $\tau \approx \kappa_d \rho h_p = 2/3$, where τ is the optical depth taken from infinity and h_p is the local scale height of the photosphere. Numerically we specify the height of the IR photosphere and compute the required incident X-ray flux.

Figure 3 shows the scale height h/R of an irradiated disk as a function of the X-ray luminosity of the central source. The X-ray luminosity is normalized to $L_{X,\text{crit}}$ from equation (4). Two representative vertical structure models ($h/R = 0.01$ and 0.5) are shown in Figure 4. In our calculations, we determine the *downscattered* X-ray flux, $F_{X,ds}$, needed to support a disk with scale height h/R . In Figure 3, this is interpreted as an X-ray luminosity of the central source using $L_X = 2 \times 4\pi R^2 F_{X,ds}(R/h)$. The factor of 2 is due to the fraction of the X-rays downscattered in the atmosphere of the disk and the factor of R/h is due to the grazing incidence of X-rays (eq. [1]). The results in Figures 3 and 4 are for a disk with a surface density of 50 g cm^{-2} around a $10^7 M_\odot$ BH at $R = 0.2 \text{ pc}$. The total column in this case is such that nearly all of the downscattered X-rays are absorbed (c.f. Figure 2). The structure of the surface layers of the disk (e.g.,

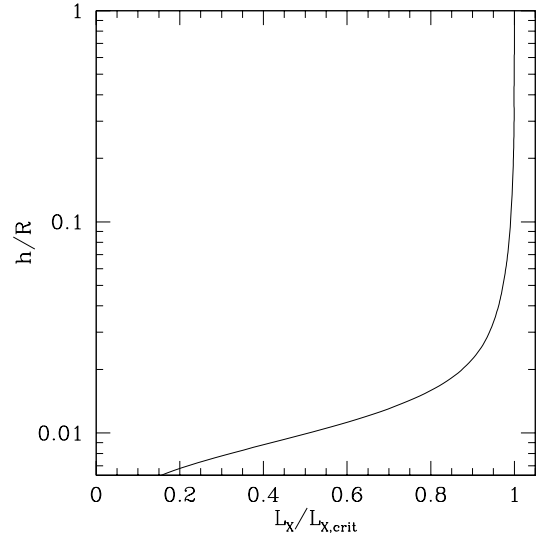


FIG. 3.— Scale height h/R of an X-ray irradiated disk as a function of the X-ray luminosity of the central source, for a disk with a surface density of 50 g cm^{-2} around a $10^7 M_\odot$ BH at $R = 0.2 \text{ pc}$. The X-ray luminosity is normalized to $L_{X,\text{crit}}$ from equation (4). We calculate vertical structure models and determine the downscattered X-ray flux $F_{X,ds}$ needed to support a disk with a scale height h/R . The required X-ray luminosity of the central source is then estimated to be $L_X = 2 \times 4\pi R^2 F_{X,ds}(R/h)$ (see the text for details). Note how a factor of 2-3 increase in L_X increases the scale-height of the disk by a factor of ~ 100 , from $h/R \approx 0.01$ to $h/R \approx 1$.

the photospheric height h) are independent of the total column once it exceeds $\approx 20 - 30 \text{ g cm}^{-2}$. Note that for the solutions shown in Figures 3 and 4, there are no internal sources of heat, such as would be provided by viscous stresses or star formation; including such internal sources of heat would lead a minimum h/R even in the absence of irradiation (unlike in our present solutions in which $h/R \rightarrow 0$ as $L_X \rightarrow 0$). This would not significantly change the properties of our solutions when $L_X \sim L_{X,\text{crit}}$.

Figure 3 shows that for $L_X \ll L_{X,\text{crit}}$, the irradiating X-rays have little effect on the structure of the disk, even in the photospheric layers: the disk remains cold and thin and is gas pressure dominated throughout. X-ray irradiation can, however, still affect the chemistry of the disk in this limit, and can lead to conditions conducive to water masing ala NGC 4258 (Maloney et al. 1996). For low accretion rates, the surface density of an AGN disk can also be sufficiently small that X-ray irradiation leads to a transition from molecular to atomic gas (e.g., Neufeld, Maloney & Conger 1994). The gas surface densities in bright AGN are, however, too large for this to occur.

For $L_X \rightarrow L_{X,\text{crit}}$, Figure 3 shows that the disk puffs up to $h \sim R$. Even in this limit, however, most of the mass remains relatively unaffected by the X-ray irradiation (e.g., the half-mass heights for the models in the left and right panels of Fig. 4 are $0.002 R$ and $0.02 R$, respectively). The transition between X-ray irradiation having relatively little dynamical effect to forcing the photosphere up to $h \sim R$ is quite abrupt, with h/R increasing by a factor of ~ 100 over only a factor of 2.5 in L_X . Physically, this is because at the temperatures of interest a gas pressure dominated disk has $h \ll R$ and only when $L_X \sim L_{X,\text{crit}}$ does radiation pressure contribute

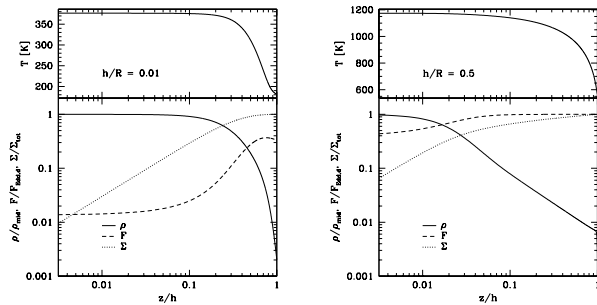


FIG. 4.— Vertical structure of an X-ray irradiated disk around a $10^7 M_\odot$ BH at $R = 0.2$ pc. The incident X-ray flux is adjusted to give $h/R = 0.01$ (left) and 0.5 (right). In the upper panel we plot the temperature as a function of height. In the lower panel we plot the density (solid line), flux (dashed line) and column (dotted line) normalized to the midplane density (ρ_{mid}), photospheric Eddington flux ($F_{\text{Edd,d}} = GMh/(R^3\kappa_d)$), and total column $\Sigma_{\text{tot}} = 50 \text{ g cm}^{-2}$, respectively. The column, Σ , is defined to be zero at the midplane. For $h/R = 0.01$, the disk is gas pressure dominated. The $h/R = 0.5$ solution, on the other hand, is radiation pressure dominated ($F/F_{\text{Edd,d}} \approx 1$) above $z/h \sim 0.05$. The half-mass heights (midplane densities) are $0.002 R$ ($n \approx 1.5 \times 10^{10} \text{ cm}^{-3}$) and $0.02 R$ ($n \approx 2 \times 10^9 \text{ cm}^{-3}$) for $h/R = 0.01$ and $h/R = 0.5$, respectively. The incident X-ray flux is $F_X \approx 3.3 \times 10^6 \text{ ergs cm}^{-2} \text{ s}^{-1}$ ($L_X/L_{\text{Edd}} \approx 0.01$) for $h/R = 0.01$ and $F_X \approx 7 \times 10^6 \text{ ergs cm}^{-2} \text{ s}^{-1}$ ($L_X/L_{\text{Edd}} \approx 0.03$) for $h/R = 0.5$.

significantly to the pressure support. Observationally, the rapid change in h/R in Figure 3 would correspond to a dramatic change in the nuclear obscuration on parsec scales for systems with $L_X \gtrsim L_{X,\text{crit}}$.

For an irradiating flux of $L_X > L_{X,\text{crit}}$, the atmosphere of the irradiated disk becomes geometrically thick and the outer layers will be blown away by a combination of the X-ray and UV radiation. Though a full wind calculation is needed to understand the dynamics of such a flow in detail, we can roughly estimate the column density through the unbound material. Since the wind is momentum driven by a super-Eddington flux, the maximum mass outflow rate is given by momentum balance, $\dot{M}_{\text{max}} v_{\text{esc}} = L/c$, where v_{esc} is the escape velocity from radius R in the disk, which gives

$$\dot{M}_{\text{max}} \sim 2.5 \left(\frac{L}{10^{44} \text{ ergs s}^{-1}} \right) R_1^{1/2} M_7^{-1/2} M_\odot \text{ yr}^{-1}, \quad (8)$$

where $R_1 = (R/1 \text{ pc})$ and $M_7 = (M_{\text{BH}}/10^7 M_\odot)$. The obscuring column through such a flow is

$$N_H \approx \frac{L}{L_{\text{Edd}}} m_p^{-1} \kappa_e^{-1} \approx 10^{24} \frac{L}{L_{\text{Edd}}} \text{ cm}^{-2}. \quad (9)$$

For typical values of L/L_{Edd} in luminous AGN, the column through the outflowing wind is Compton-thin with $N_H \approx 10^{22} - 10^{23} \text{ cm}^{-2}$. Equations (8) and (9) assume that all of the luminosity of the central source contributes to driving an outflow. This is not correct for the X-ray flux, since the resulting column is Compton thin. However, once the photosphere of the disk is moderately inflated by X-ray irradiation, the UV flux will become dynamically important and will also contribute to unbinding the surface layers of the disk. Thus the above estimates of the mass loss rate and column are likely to be reasonable.

3. DUST GRAIN GROWTH IN AGN DISKS

As discussed in the previous section, the impact of the X-ray and UV radiation from a central AGN on its surrounding accretion disk depends sensitively on the FIR opacity of the disk. For temperatures of $\sim 300 - 10^3 \text{ K}$, typical models of ISM dust have opacities of $5 - 15 \text{ cm}^2 \text{ g}^{-1}$. We now argue that this opacity may be enhanced in the near-AGN environment due to 1. supersolar metallicity and 2. larger dust grains.

If most metals are locked up into dust, enhancements in the metallicity increase the opacity as Z/Z_\odot . From quasar observations, the broad line region appears to have metallicities that are a few to ten times solar (Hamann & Ferland 1999; Baldwin et al. 2003; Dietrich et al. 2003; Nagao, Marconi, & Maiolino 2006). Note that these metallicities probe just the central nuclear regions of AGN, whose chemical evolution might be significantly different from the host galaxy (Hamann & Ferland 1999). In addition recent work on the narrow line region of Seyferts and AGN outflows show supersolar metallicity (Groves, Heckman & Kauffmann 2006; Arav et al. 2006). For Draine's (2003) Rosseland mean opacity of $\kappa_d \approx 15 \text{ cm}^2 \text{ g}^{-1}$, a metallicity enhancement at the level of 2-4 would increase κ_d to $\approx 30 - 60 \text{ cm}^2 \text{ g}^{-1}$. This corresponds to $\kappa_e/\kappa_d \approx 10^{-2}$, in which case AGN with X-ray luminosities $\gtrsim 0.01 - 0.03 L_{\text{Edd}}$ will have an X-ray flux that is super-Eddington with respect to the dust on parsec scales.

An independent argument for enhanced FIR opacity in small-scale AGN disks is that the dust grains may preferentially be larger than in the local ISM. We begin by considering the observational lines of evidence for (and against) this conclusion. Recent detections of the $10 \mu\text{m}$ silicate emission feature in AGN find that the emission feature is broadened and shifted to slightly longer wavelengths than in the ISM (Siebenmorgen et al. 2005; Hao et al. 2005; Sturm et al. 2005). This is analogous to the emission features in Herbig Ae/Be systems (Bouwman et al 2001) and may indicate different dust properties, in particular larger or more amorphous grains. On the other hand, the silicate absorption features in Type 2 AGN do not appear to require unusual dust properties, but may require a patchy distribution of dust (Roche et al. 1991; Hao et al. 2007; Levenson et al. 2007). Additional constraints on the properties of dust in the vicinity of AGN can be provided by extinction measurements. Maiolino et al. (2001ab) used such measurements to argue that dust grains near AGN may be significantly larger than interstellar medium grains. Similarly, Gaskell et al. (2004) argue that the reddening law near AGN is substantially different from any standard reddening law and that the minimum size for dust grains in the near-AGN environment is $a \approx 0.3 \mu\text{m}$ due to a lack of reddening in the UV. Using SDSS data on a large number of AGN, however, Hopkins et al. (2004) argue against such a Gaskell-like reddening law, and in favor of SMC-like dust.

Although the observational arguments for larger dust grains near AGN are by no means conclusive, there are theoretical arguments for this conclusion as well. To show this, we consider the evolution of dust grains in AGN disks via accretion of metals from the gas and dust grain coagulation. Lacking a detailed model for the ISM on parsec scales near AGN, we make two simplifying assumptions. First, we assume that grain growth is im-

portant if it occurs on a timescale less than the local dynamical time $t_{\text{dyn}} \sim \Omega^{-1} \sim 5000 R_1^{3/2} M_7^{-1/2}$ yrs. The dynamical time is comparable to the eddy turnover time on the outer-scale, which is \sim the timescale on which dust would be destroyed by shocks if turbulence is supersonic in the disk. Our second simplifying assumption is that we estimate the gas density in the disk ρ_g in terms of the Toomre Q parameter for gravitational stability, via $\rho_g = M_{BH} Q^{-1} / (2\pi R^3) \rightarrow n \approx 6 \times 10^7 Q^{-1} M_7 R_1^{-3} \text{ cm}^{-3}$. We assume $Q \sim 1$, as suggested by theoretical arguments (e.g., Sirko & Goodman 2003; Thompson et al. 2005) and as is observed in a diverse range of galaxies from local spirals (e.g., Martin & Kennicutt 2001) to luminous starbursts (e.g., Downes & Solomon 1998). Although the ISM in the vicinity of AGN undoubtedly consists of multiple phases, $Q \sim 1$ should provide a reasonable guide to the mean ISM densities. The gas densities implied by $Q \sim 1$ are also consistent with the densities of $\approx 10^7 - 10^{10} \text{ cm}^{-3}$ required to account for the observed water maser emission from the central parsecs of a number of AGN (see, e.g., Lo 2005 for a review).

We begin by considering the timescale for a dust grain to grow appreciably in mass via accretion of gas-phase metals, which is

$$t_{\text{acc}} \sim \frac{m_d}{\rho_m \sigma v_m} \approx \frac{4}{3} \frac{a \rho_d}{v_m \rho_m} \approx 100 \frac{a_1 \rho_{d,3} R_1^3 Q}{T_3^{1/2} M_7} \text{ yrs} \ll t_{\text{dyn}} \quad (10)$$

where $m_d = \rho_d 4\pi a^3 / 3$ is the mass of the dust grain, $\sigma = \pi a^2$ is the dust-gas collision cross section, $v_m \approx 1 T_3^{1/2} \text{ km s}^{-1}$ is the thermal velocity of the metals at temperature $10^3 T_3 \text{ K}$ (assuming $A \sim 20$), $\rho_d = 3 \rho_{d,3} \text{ g cm}^{-3}$ is the dust grain density, $a = a_1 \mu\text{m}$ is the radius of the dust grain, and $\rho_m \approx 0.01 \rho_g$ is the mass density in metals. Note that we take a standard dust grain density of 3 g cm^{-3} . Equation (10) shows that dust grains can increase their mass on a timescale significantly less than the local dynamical time. Thus even if some grains (or their mantles) are destroyed, the free metals accrete onto remaining dust quite rapidly.

The high gas densities in AGN disks also make them a promising environment for grain coagulation, as is inferred to occur in protostellar disks (van Boekel et al. 2003). To show this, we estimate the characteristic velocity dispersion of dust grains and show that a significant fraction of small dust grains stick on impact. The timescale for coagulation is of order the dynamical time so this process occurs quickly.

We begin by estimating the velocity dispersion of grains in a turbulent medium following the argument given by Draine (1985). The velocity dispersion of grains is determined by the scale on which the eddy turnover time, t_{eddy} , is comparable to the aerodynamic drag timescale, t_{drag} , for grains in gas. The latter timescale is given by

$$t_{\text{drag}} \sim \frac{m_d}{\rho_g \sigma c_s} \sim 8 \times 10^6 \rho_{d,3} R_1^3 M_7^{-1} T_3^{-1/2} a_1 Q \text{ s}, \quad (11)$$

where c_s is the thermal velocity of the gas. On the largest scales, the accretion disk possesses a turbulent velocity approaching h/R times the orbital velocity, v_{orb} . As in the ISM, these velocities are likely supersonic compared

to the gas sound speed and so we assume a supersonic cascade with $v_{\text{eddy}} \sim (h/R) v_{\text{orb}} (l_{\text{eddy}}/h)^{1/2}$, where l_{eddy} is the size scale of the eddy. The eddy turnover time, t_{eddy} , is given by

$$t_{\text{eddy}} \sim t_{\text{dyn}} \left(\frac{l_{\text{eddy}}}{h} \right)^{1/2}. \quad (12)$$

As turbulence cascades to smaller and smaller scales, the eddy velocities decrease. Eventually, $v_{\text{eddy}} \sim c_s$ and turbulence transitions from supersonic to subsonic. We define the eddy turnover time at this scale (when $v_{\text{eddy}} = c_s$) as the sonic time, t_{sonic} , which is given by

$$t_{\text{sonic}} \sim t_{\text{dyn}} \frac{R}{h} \frac{c_s}{v_{\text{orb}}} \approx 100 T_3^{1/2} M_7^{-1} R_1^2 \left(\frac{h}{R} \right)^{-1} \text{ yrs} \quad (13)$$

The sonic time is still much longer than t_{drag} , so that the dust responds coherently to the eddy. Below this scale, we assume that the turbulence is subsonic and incompressible so that it adopts a Kolmogorov spectrum. This assumption is conservative in the sense that continuing the $l^{1/2}$ scaling of supersonic turbulence to smaller scales would result in smaller grain velocities and thus a higher probability of dust sticking. For the Kolmogorov cascade, the velocities of the turbulent eddies scale like $v_{\text{eddy}} \sim c_s (l/l_{\text{sonic}})^{1/3}$, where l_{sonic} is the length-scale of eddies with turnover times of t_{sonic} . The velocity of eddies with $l < l_{\text{sonic}}$ or $t < t_{\text{sonic}}$ is

$$v_{\text{eddy}} \sim c_s \left(\frac{l_{\text{eddy}}}{l_{\text{sonic}}} \right)^{1/3} \sim c_s \left(\frac{t_{\text{eddy}}}{t_{\text{sonic}}} \right)^{1/2}. \quad (14)$$

The most important eddies are those with $t_{\text{eddy}} \sim t_{\text{drag}}$. For $t_{\text{eddy}} \ll t_{\text{drag}}$, the dust does not respond to the eddy. In the opposite extreme, $t_{\text{eddy}} \gg t_{\text{drag}}$, all local dust particles will attain a net coherent motion. Hence the local random velocity of dust particles is set by the scale on which $t_{\text{eddy}} \sim t_{\text{drag}}$, i.e.,

$$v_d \sim c_s \left(\frac{t_{\text{drag}}}{t_{\text{sonic}}} \right)^{1/2} \sim 200 R_1^{1/2} \rho_{d,3}^{1/2} a_1^{1/2} \left(\frac{h}{R} \right)^{1/2} Q^{1/2} \text{ m s}^{-1}. \quad (15)$$

Numerical experiments indicate that dust grains that approach one another at $\lesssim 10 \text{ m/s}$ will stick to each other (Pope, Blum, & Henning 2000), while at much higher velocities $\sim 1 \text{ km s}^{-1}$ they are destroyed on impact.

The thickness of the accretion disk in AGN is uncertain. Models predict $h/R \sim 0.1 - 10^{-3}$ on \sim parsec scales (e.g., Thompson et al. 2005), although this depends on the uncertain viscosity in the disk. Taking $h/R \sim 10^{-2}$, we find that the velocity dispersion for μm -sized dust grains is $\sim 20 \text{ m s}^{-1}$. Due to the $a^{1/2}$ scaling for the random velocity from equation (15), coagulation is more likely for smaller grains, while fragmentation becomes more likely for larger grains. In the previous section we showed that irradiation can extend the photosphere of the disk up to a height of $\sim R$. However, most of the mass of the disk is still contained in a thin layer with $h/R \ll 1$ (see § 3). Thus the above argument about coagulation remains valid for most of the mass.

We can estimate the timescale for dust coagulation by considering the fraction of dust grains which approach

each other with a low enough velocity such that they will stick (e.g., Chakrabarti & McKee 2005). For this population, the coagulation timescale is

$$\frac{t_{\text{coag}}}{t_{\text{dyn}}} \sim 1 R_1^{3/2} M_7^{-1/2} a_1 f \left(\frac{v}{10 \text{ m s}^{-1}} \right)^{-1} Q \rho_{d,3}, \quad (16)$$

where f is the fraction of the dust particle population with $v \sim 10 \text{ m s}^{-1}$. The dust coagulation timescale is roughly the dynamical time for $1 \mu\text{m}$ grains and much shorter for submicron-sized grains. Hence it is likely that a significant fraction of the dust grains in AGN disks will coagulate to form larger grains. As a check on our reasoning, equation (16) can be scaled to conditions appropriate to proto-stellar disks. For $M \sim 1 M_\odot$, $R \sim 200 \text{ A.U.}$, and $Q \sim 10$ (Andrews & William 2007), we find $t_{\text{coag}}/t_{\text{dyn}} \sim 1$, similar to our result for AGN disks. Submm observations which probe dust emission from the outer parts of protostellar disks indeed find evidence for significant grain growth, consistent with the inference from equation (16) (Draine 2006; Andrews & Williams 2007).

In the ISM of the Milky Way, the timescale for dust to be destroyed by supernova shocks is significantly shorter than the timescale on which dust is injected by star formation (e.g., Jones et al. 1994). Thus grain growth in the interstellar medium appears crucial for establishing the observed properties of Galactic dust (e.g., the size distribution). We suspect that a similar balance between grain growth (argued for above) and grain destruction will set the grain size properties in AGN disks. In the vicinity of AGN the intense radiation field, thermal sputtering by hot gas, and shock processing of grains all likely contribute to grain destruction, and preferentially destroy smaller dust grains (e.g., Laor & Draine 1993). Accurately estimating the grain destruction time is clearly difficult given the poor understanding of the physical conditions in parsec-scale AGN disks. As a plausible order of magnitude estimate we note that if the AGN disk is supersonically turbulent on scales where self-gravity is important (as in the Milky Way), dust will typically encounter a supersonic shock once every dynamical time. During such encounters, dust grain are either broken up or have their outer parts vaporized. Freed metals quickly recondense (eq. [10]) and small dust particles coagulate (eq. [16]). Equation (16) implies that coagulation depends on dust grain size, with $t_{\text{coag}} \sim t_{\text{dyn}}$ for $a \sim 1 \mu\text{m}$ on parsec scales. If the dust destruction time is indeed $\sim t_{\text{dyn}}$, this suggests that the AGN environment tends to favor the production of μm -sized dust grains, although this is clearly uncertain at the factor of a few level.

If a significant fraction of the dust mass is contained in grains with sizes of $\sim 1 \mu\text{m}$ the FIR opacity will be enhanced, increasing the importance of the irradiating X-ray and UV flux. For a spherical dust grain with radius a , the opacity is maximized when $\pi a \sim \lambda$, where a is the size of the dust grain and λ is the wavelength of interest. At $T \approx 500 \text{ K}$, $\lambda \approx 6 \mu\text{m}$ and therefore the dust opacity is maximized for grains with $a \approx 2 \mu\text{m}$. When the opacity is maximized, the cross section of the dust grain is close to geometric, so that the opacity is given by

$$\kappa_d = \frac{\pi a^2 f_d}{4/3 \pi \rho_d a^3} \approx 25 a_1^{-1} \rho_{d,3}^{-1} \left(\frac{f_d}{0.01} \right) \text{ cm}^2 \text{ g}^{-1}, \quad (17)$$

where $f_d \approx 1\%$ (for solar metallicity) is the dust mass to gas ratio, and as discussed above, κ_d increases roughly linearly with Z/Z_\odot . Note that we have assumed a standard dust grain density is $\rho = 3 \text{ g cm}^{-3}$. Large dust grains are likely full of holes and voids, lowering the density and raising the opacity. Equation (17) implies a FIR opacity up to a factor of few-5 times larger than in the Milky Way (independent of any enhancement to the opacity due to supersolar metallicity).

4. DISCUSSION AND CONCLUSIONS

In the presence of a sufficient irradiating X-ray flux, the outer atmosphere of an initially thin AGN disk puffs up into a geometrically thick configuration that provides significant obscuration along most lines of sight. We estimate that for $L_X \gtrsim L_{X,\text{crit}} \approx 0.01 - 0.1 L_{\text{Edd}}$ X-ray heating is dynamically important for the structure of AGN disks on parsec scales; the upper end of this range is appropriate for normal ISM dust, while the lower end of the range is appropriate if, as we have argued, the FIR opacity in AGN disks is enhanced through a combination of supersolar metallicities and grain growth (§4). The latter may occur in AGN disks on parsec scales in direct analogy with massive protostellar disks.

For $L_X < L_{X,\text{crit}}$, irradiation has little dynamical effect on the properties of AGN disks, while for $L_X > L_{X,\text{crit}}$, X-ray heating likely drives a significant outflow from the surface of the underlying accretion disk. The transition between these two different regimes is very abrupt with h/R increasing by a factor of ~ 100 with a factor of ≈ 2.5 increase in X-ray flux (Fig. 3). Our results thus predict a marked increase in the presence of small-scale nuclear obscuration for the most X-ray luminous AGN. This obscuring material should preferentially lie at distances of $\sim 0.1 - 3 \text{ pc}$ from the central AGN because outside $\sim 3 M_7^{1/2} \text{ pc}$ the bulge mass dominates the BH mass and so the irradiating flux is less likely to be locally super-Eddington. Grain growth, if it occurs, also occurs preferentially at radii of $\sim 0.1 - 1 \text{ pc}$. Using the estimated mass loss rate in a continuum radiation pressure driven wind, we find characteristic obscuring columns of $\sim 10^{22-23} \text{ cm}^{-2}$ for luminous AGN, in reasonable agreement with observations (e.g., Risaliti, Maiolino & Salvati 1999). Without a more sophisticated model, however, it is difficult to quantitatively determine the solid angle subtended by this material, although we expect it to be $\sim \pi$, implying a significant fraction of Type 2 AGN even at high luminosities. This is consistent with, e.g., the implied covering fraction of dusty material of $\approx 10 - 50\%$ from the IR fluxes of unobscured Type 1 quasars.

Luminous Seyferts and quasars have X-ray Eddington ratios in the range required for X-ray irradiation to be dynamically important. This is particularly true if the FIR opacity is enhanced in AGN disks. In a sample of 35 reverberation mapped AGN, Peterson et al. (2004) found that a significant fraction had $L_{\text{Bol}} \gtrsim 0.1 L_{\text{Edd}}$. Taking into account the X-ray emission up to $\sim 100 \text{ keV}$, Seyferts typically have $L_X/L_{\text{Bol}} \sim 0.1 - 0.3$ (e.g., Marconi et al. 2004), and so we expect quite a few systems will have X-ray fluxes that are super-Eddington with respect to the dust in a parsec-scale disk. At high redshift, bolometric Eddington ratios for luminous AGN are $\approx 1/3 - 1$ (e.g., Kollmeier et al. 2006), although quasars

emit a smaller fraction of their flux in the X-ray than do Seyferts (e.g., Elvis et al. 1994; Marconi et al. 2004) and so their X-ray Eddington ratios are similar.

We now discuss our model in the context of observations of few specific systems. INTEGRAL observations directly probe the high energy emission from AGN that dominates the Compton heating of surrounding material. To focus on a concrete example, the Seyfert 2 galaxy NGC 4388 has an X-ray luminosity of $L_X \approx 4 \times 10^{43} \text{ ergs s}^{-1}$ between 20 – 100 keV and is Compton thin with $N_H \approx 3 \times 10^{23} \text{ cm}^{-2}$ (Beckman et al. 2006). NGC 4388 has a central BH mass of $M_{\text{BH}} \approx 6 \times 10^6 M_\odot$ (Woo & Urry 2002), which implies $L_X/L_{\text{Edd}} \approx 0.04$. This X-ray Eddington ratio and the observed obscuring column are consistent with our results on the effect of radiation pressure on parsec-scale disks in AGN.

To consider another concrete example, the prototypical Seyfert 2 NGC 1068 is believed to be radiating at roughly a third of Eddington (Ho 2002; Pounds & Vaughan 2006). The inferred X-ray Eddington ratio for 1068 is $L_X/L_{\text{Edd}} \approx 0.01$ (e.g., Panessa et al. 2006), but this is extremely uncertain because 1068 is Compton thick. For reasonable intrinsic X-ray Eddington ratios, the X-ray flux of NGC 1068 is quite likely to be dynamically important for the surrounding material. Infrared interferometry of NGC 1068 at $8.7 \mu\text{m}$ by Jaffe et al. (2004) reveals the presence of a hot optically thick dust component ($T > 800 \text{ K}$) 0.7 pc from the black hole with a scale height of $h/R > 0.6$. The spatial scale and geometric structure of this obscuring material are consistent with the predictions of our model. However, the obscuring column in 1068 exceeds our nominal prediction of $\sim 10^{22} - 10^{23} \text{ cm}^{-2}$. In our models, larger columns would be observed at low inclination when the line of sight passes through the denser parts of the disks's atmosphere (see Fig. 4).

Although radiation pressure is likely to be dynamically significant in shaping the observed properties of obscuring material in luminous AGN, it is equally clear that there are a number of systems in which this is not the case. In particular, low luminosity AGN such as NGC 4258 (Greenhill et al. 1995) and NGC 3227 (Davies et al. 2006) are far too sub-Eddington for irradiation to be important. In such systems, other modes of obscuration are likely important, perhaps including a warped disk, obscuration by the host galaxy (e.g. MCG-6-30-15; Balantyne, Weingartner, & Murray 2003), an accretion disk outflow, or inflowing molecular clouds. Our prediction is that luminous AGN should preferentially have a very compact source of nuclear obscuration that is intrinsically geometrically thick (in contrast to a warped disk). Continued progress on IR interferometry should allow better observational probes of the spatial scale of nuclear obscuration in AGN. Continuum reverberation mapping

between the IR and optical in a sample of Seyfert 1s already provides evidence that the obscuring material extends down to the sublimation radius in many systems (e.g., Suganuma et al. 2006).

Our calculations have shown that geometrically thin disks on parsec scales in luminous AGN are likely to be substantially modified by X-ray irradiation. Once the surface layers of the disk start to become geometrically thick, UV heating will become dynamically important as well. Since the UV luminosity is larger than the X-ray luminosity, UV irradiation will ultimately have a significant effect on the structure of the geometrically thick obscuring material (as in Pier & Krolik 1992), although the X-rays will likely, as we have argued, play the key role in initially thickening this material. A proper treatment of the structure of the irradiated parsec-scale disk thus ultimately demands a self-consistent multi-dimensional calculation that is beyond the scope of this work (see Krolik 2006 for axisymmetric hydrostatic calculations of radiation pressure supported tori). In light of these uncertainties, the mass outflow rate (eq. [8]) and obscuring column (eq. [9]) estimated in §3 can only provide an order of magnitude guide to the mass and column supported by irradiation. Another over-simplification in our calculation is that we have modeled the disk as a uniform medium, which is probably not a good approximation. In addition to clumping due to self-gravity, radiation supported atmospheres and winds are subject to instabilities that amplify inhomogeneities (e.g., Rayleigh-Taylor and photon bubble instabilities). This may increase the typical obscuring column at fixed \dot{M} relative to that estimated in equation (9). Finally, we note that the mass outflow rate driven by radiation pressure (eq. [8]) may be substantial relative to the accretion rate onto the central black hole. This supports the hypothesis (e.g., Murray, Quataert, & Thompson 2005) that feedback from radiation pressure can help regulate the growth of supermassive black holes in galactic nuclei.

We thank the referee, Bruce Draine, for a thorough reading and making many suggestions which greatly improved this paper. We thank R. Antonucci, S. W. Davis, J. Krolik, A. Socrates, and T. Thompson for detailed discussions. We thank J. Weingartner for sharing his numerical calculations on dust opacity. We thank S. Chakrabarti for pointing out the importance of grain growth. We also thank S. Andrews and J. Williams for providing a preprint of their paper. P. C. was supported by the Miller Institute for Basic Research. E. Q. was supported in part by NASA grant NNG05GO22H, an Alfred P. Sloan Fellowship, and the David and Lucile Packard Foundation. N. M. is supported by NSERC of Canada

REFERENCES

- Andrews, S. M. & Williams, J. P. 2007, submitted to ApJ
 Antonucci, S. 1993, ARA&A, 31, 473
 Arav, N., Gabel, J. R., Korista, K. T., Kaastra, J. S., Kriss, G. A., Behar, E., Costantini, E., Gaskell, C. M., Laor, A., Koditwakkhu, N., Proga, D., Sako, M., Scott, J. E., & Steenbrugge, K. C. 2006, *to appear in ApJ*, astro-ph/0611928
 Baldwin, J. A., Hamann, F., Korista, K. T.; Ferland, G. J., Dietrich, M., & Warner, C. 2003, ApJ, 583, 649
 Ballantyne, D. R., Weingartner, J. C., & Murray, N. 2003, A&A, 409, 503
 Beckmann, V., Gehrels, N., Shrader, C. R., & Soldi, S. 2006, ApJ, 638, 642
 Bouwman, J., Meeus, G. de Koter, A., Hony, S., Dominik, C., & Waters, L. B. F. M. 2001, A&A, 375, 950
 Chakrabarti, S. & McKee, C. F. 2005, ApJ, 631, 792
 Davies, R., Thomas, J., Genzel, R., Sanchez, F. M., Tacconi, L., Sternberg, A., Eisenhauer, F., Abuter, R., Saglia, R., & Bender, R. 2006, *accepted by ApJ*, astro-ph/0604125
 Dietrich, M., Hamann, F., Shields, J. C., Constantin, A., Heidt, J., Jager, K., Vestergaard, M., & Wagner, S. J. 2003, ApJ, 589, 722

- Downes, D. & Solomon, P. M. 1998, *ApJ*, 507, 615
- Draine, B. T. 1985 in *Protostars and Planets II*, ed. D. C. Black & M. S. Matthews (Tucson: Univ. Arizona Press), 621
- Draine, B. T. 2003, *ARA&A*, 41, 241
- Draine, B. T. 2006, *ApJ*, 636, 1114
- Elvis, M., Wilkes, B. J., McDowell, J. C.; Green, R. F., Bechtold, J., Willner, S. P., Oey, M. S.; Polomski, E., Cutri, R. 1994, *ApJS*, 95, 1
- Gaskell, C. M, Goosmann, R. W., Antonucci, R. R. J., & Whysong, D. H. 2004, *ApJ*, 616, 147
- Greenhill, L. J., Jiang, D. R., Moran, J. M., Reid, M. J., Lo, K. Y., & Claussen, M. J. 1995, *ApJ*, 440, 619
- Groves, B., Heckman, T., Kauffmann, G. 2006, *accepted by MNRAS*, astro-ph/0607311
- Hamann, F. & Ferland, G. 1999, *ARA&A*, 37, 487
- Hao, L. et al. 2005, *ApJ*, 625, L75
- Hao, Lei, Weedman, D. W., Spoon, H. W. W., Marshall, J. A., Levenson, N. A., Elitzur, M., & Houck, J. R. 2007, *ApJ*, 655, L77
- Ho, L. C. 2002, *ApJ*, 564, 120
- Hopkins, P. F., Strauss, M. A.; Hall, P. B.; Richards, G. T., Cooper, A. S., Schneider, D. P., Vanden Berk, D. E., Jester, S., Brinkmann, J., Szokoly, G. P. 2004, *AJ*, 128, 1112
- Jaffe, W. et al. 2004, *Nature*, 429, 47
- Jones, A. P., Tielens, A. G. G. M., Hollenbach, D. J., & McKee, C. F. 1994, *ApJ*, 433, 797
- Kollmeier, J. A., Onken, C. A., Kochanek, C. S., Gould, A., Weinberg, D. H., Dietrich, M., Cool, R., Dey, A., Eisenstein, D. J., Jannuzi, B. T., Le Floch, E., Stern, D. 2006, *ApJ*, 648, 128
- Konigl, A. & Kartje, J. F. 1994, *ApJ*, 434, 446
- Krolik, J. & Begelman, M. C. 1988, *ApJ*, 329, 702
- Krolik, J., 2006, submitted to *ApJ*
- Laor, A. & Draine, B. T. 1993, *ApJ*, 402, 441
- Levenson, N. A., Sirocky, M. M., Hao, L., Spoon, H. W. W., Marshall, J. A., Elitzur, M., & Houck, J. R. 2007, *ApJ*, 654, L45
- Lo, K. Y. 2005, *ARA&A*, 43, 625
- Maiolino, R., Marconi, A., Salvati, M., Risaliti, G., Severgnini, P., Oliva, E., La Franca, F., & Vanzi, L. 2001a, *A&A*, 365, 28
- Maiolino, R., Marconi, A., Salvati, M., Risaliti, G., Severgnini, P., Oliva, E., La Franca, F., & Vanzi, L. 2001b, *A&A*, 365, 37
- Maloney, P. R., Hollenbach, D. J. & Tielens, A. G. G. M. 1996, *ApJ*, 466, 561
- Marconi, A., Risaliti, G., Gilli, R., Hunt, L. K., Maiolino, R., Salvati, M. 2004, *MNRAS*, 351, 169
- Martin, C. L. Kennicutt, R. C. Jr. 2001, *ApJ*, 555, 301
- Murray, N., Quataert, E., & Thompson, T. A. 2005, *ApJ*, 618, 569
- Nagao, T., Marconi, A., & Maiolino, R. 2006, *A&A*, 447, 157
- Neufeld, D. A.; Maloney, P. R.; Conger, S. 1994, *ApJ*, 436, L127
- Panessa, F., Bassani, L., Cappi, M., Dadina, M., Barcons, X., Carrera, F. J., Ho, L. C., Iwasawa, K. 2006, *accepted by A&A*, astro-ph/0605236
- Peterson, B. M. et al. 2004, *ApJ*, 613, 682
- Pier, E. A. & Krolik, J. H. 1992, *ApJ*, 399, L23
- Poppe, T., Blum, J., & Henning, T. 2000, *ApJ*, 533, 472
- Pounds, K. & Vaughan, S. 2006, *MNRAS*, 368, 707
- Ptak, A., Zakamska, N. L., Strauss, M. A., Krolik, J. H., Heckman, T. M., Schneider, D. P., Brinkmann, J. 2006, *ApJ*, 637, 147
- Risaliti, G., Maiolino, R., & Salvati, M. 1999, *ApJ*, 522, 157
- Roche, P. F., Aitken, D. K., Smith, C. H., & Ward, M. J. 1991, *MNRAS*, 248, 606
- Sanders, D. B., Phinney, E. S., Neugebauer, G., Soifer, B. T., & Matthews, K. 1989, *ApJ*, 347, 29
- Semenov, D., Henning, T., Helling, C. Ilgner, M., & Sedlmayr, E. 2003, *A&A*, 410, 611
- Siebenmorgen, R., Haas, M., Krugel, E., & Schulz, B. 2005, *A&A*, 436, L5
- Sirko, E. & Goodman, J. 2003, *MNRAS*, 341, 501
- Suganuma, M., et al. 2006, *ApJ*, 639, 46
- Sturm, E. et al 2005, *ApJ*, 629, L21
- Thompson, T.A., Quataert, E., & Murray, N. 2005, *ApJ*, 630, 167
- van Boekel, R., Waters, L. B. F. M., Dominik, C., Bouwman, J., de Koter, A., Dullemond, C. P., & Paresce, F. 2003, *A&A*, 400, L21
- Wada, K., & Norman, C. A. 2002, *ApJ*, 566, L21
- Woo, J.-H. & Urry, C. M. 2002, *ApJ*, 579, 530
- Zakamska, N. L. et al. 2003, *AJ*, 126, 2125
- Zakamska, N. L. et al. 2005, *AJ*, 129, 1212